

# Positioning Error Probability for Some Forms of Center-of-Gravity Algorithms Calculated with the Cumulative Distributions. Part I.

Gregorio Landi<sup>a\*</sup>, Giovanni E. Landi<sup>b</sup>

<sup>a</sup> Dipartimento di Fisica e Astronomia, Universita' di Firenze and INFN  
Largo E. Fermi 2 (Arcetri) 50125, Firenze, Italy

<sup>b</sup> ArchonVR S.a.g.l.,  
Via Cisieri 3, 6900 Lugano, Switzerland.

June 1, 2020

## Abstract

To complete a previous paper, the probability density functions of the center-of-gravity as positioning algorithm are derived with classical methods. These methods, as suggested by the textbook of Probability, require the preliminary calculation of the cumulative distribution functions. They are more complicated than those previously used for these tasks. In any case, the cumulative probability distributions could be useful. The combinations of random variables are those essential for track fitting  $x = \xi/(\xi + \eta)$ ,  $x = \theta(x_3 - x_1)(-x_3)/(x_3 + x_2) + \theta(x_1 - x_3)x_1/(x_1 + x_2)$  and  $x = (x_1 - x_3)/(x_1 + x_2 + x_3)$ . The first combination is a partial form of the two strip center-of-gravity. The second is the complete form, and the third is a simplified form of the three strip center-of-gravity. The cumulative probability distribution of the first expression was reported in the previous publications. The standard assumption is that  $\xi$ ,  $\eta$ ,  $x_1$ ,  $x_2$  and  $x_3$  are independent random variables.

## Contents

<b>1</b>	<b>Introduction</b>	<b>2</b>
<b>2</b>	<b>Simple two strip case</b>	<b>2</b>
2.1	Probability Density Function . . . . .	6
2.2	Cumulative probability using the left strip . . . . .	6
<b>3</b>	<b>The complete two strip center-of-gravity</b>	<b>7</b>
<b>4</b>	<b>Three strip COG probability distribution</b>	<b>10</b>
4.1	Expression with Gaussian additive noise and few plots . . . . .	14
<b>5</b>	<b>Conclusions</b>	<b>15</b>

---

\*Corresponding author. Gregorio.Landi@fi.infn.it

# 1 Introduction

In reference [1], the probability density functions (PDFs) of positioning errors for some forms of Center-of-Gravity (COG) algorithms were reported. Their derivations were obtained with a straightforward methods, the Fermi golden rule #1, an usual tool to handle hard constraints in quantum mechanics. Of those PDFs, only one was derived with the standard textbook method (for example [2]) through the calculation of the cumulative probability function. This type of derivation was heavily synthesized in an appendix of ref. [1]. Here, our aim is to use the textbook-style calculation for the other two most important COG algorithms: the complete two-strip COG and the simple three-strip COG. In any reference to these PDFs, we stated that our first developments were with the calculations of the cumulative probability and its successive differentiation, thus, we report them in the following. We never used the cumulative probability functions in our track reconstructions, but we can not exclude their possible utility. However, we encountered a hard animosity against our approaches that suggests us to be redundant to avoid criticisms. For example, to counteract the criticisms of our readers we had to produce two different demonstrations (refs. [3, 4]) about the superiority of our fitting methods compared the standard ones. We supposed, as usual, that a set of simulations suffices. Instead very complex and length demonstrations were pretended as *condition sine qua non* for the publication of ref. [5]. We rejected this pretense considering that as substantial distortion of ref. [5], without no additional contribution to our results. In our plans, ref. [5] was a phenomenological discussion of two of our unexpected results, the linear growth and the lucky model, without resorting to long equations. In any case, refs. [3, 4] contain all the equations missed to ref. [5] (for the referee point of view). The PDFs, derived here and in ref. [1], are one of the key elements of our approach of refs. [6, 7]. The other key element is the theorem of ref. [6], this is essential to insert the functional dependence from the impact point in the PDFs. In fact, it is the estimation of the track impact points the aim of all these developments. Figures 15 and 16 of ref. [6] illustrate very well the ability of these methods to estimate the track impact points and the unexpected importance of the Cauchy-(Agnesi) tails. A detailed discussion of the use of the theorem of ref. [6] to complete the PDFs with the functions of the track impact points will be the subject of a future paper. When we started this study of the COG PDFs, we expected that a large part of these developments were well known, the COG algorithms are in use by a long time. With our surprise, we discovered that nobody worried to calculate them. The belief that all the probabilities are Gaussian functions is very hard to die. The perception to move in an unexplored land obliged us to pay attention to any detail and to select the best allowed path. This strategy was very rewarding, producing good expected outcomes and excellent unexpected results. The following are our original `LaTeX`-notes where we suppressed the parts reported in ref. [1]. The last subsection contains figures of the PDFs for three strip COG compared with the PDFs for two strip COG.

## 2 Simple two strip case

Now we calculate the cumulative probability of a simple two-strip COG, extending the compressed discussion of ref [1]. The parameters of the problem are the two energies collected by adjacent strips, each one affected by an additive random noise (probably Gaussian as our data look to support). We will proceeds along the lines of the application of ref. [2] to a ratio of two random variables. In our case we have two random variables but the ratio is that of a COG  $\xi/(\xi + \eta)$ . As in ref. [2] we will consider the regions where:

$$F_2(x) = P\left(\frac{\xi}{\xi + \eta} \leq x\right) \quad (1)$$

The derivative of Eq. 1 respect to  $x$  gives the PDF of this case. We have first two conditions:

- $\xi + \eta \geq 0$
- $\xi + \eta < 0$

The plane  $(\eta, \xi)$  is divided in two parts by the line  $\xi = -\eta$  (figure 1).

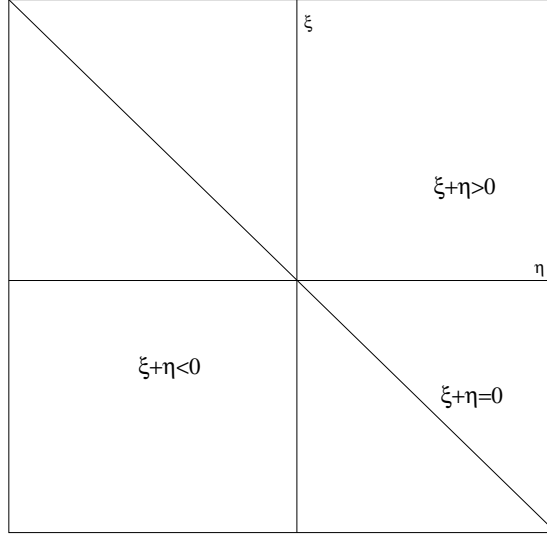


Figure 1: Sector of the plane  $(\eta, \xi)$  where  $\xi + \eta > 0$  or  $\xi + \eta < 0$  and its boundary  $\xi + \eta = 0$

We have various conditions to satisfy to find  $F_2(x)$ .

$$\begin{aligned} \frac{\xi}{\xi + \eta} < x \rightarrow \xi + \eta > 0 \Rightarrow \xi < x(\xi + \eta) \Rightarrow \xi(1-x) < x\eta \\ x < 0 \Rightarrow \xi \frac{(1-x)}{x} > \eta \quad x > 0 \Rightarrow \xi \frac{(1-x)}{x} < \eta \end{aligned} \quad (2)$$

and similarly we have:

$$\begin{aligned} \frac{\xi}{\xi + \eta} < x \rightarrow \xi + \eta < 0 \Rightarrow \xi > x(\xi + \eta) \Rightarrow \xi(1-x) > x\eta \\ x < 0 \Rightarrow \xi \frac{(1-x)}{x} < \eta \quad x > 0 \Rightarrow \xi \frac{(1-x)}{x} > \eta \end{aligned} \quad (3)$$

From the definition of  $x$ , we see that the equation  $\xi = 0$  is obtained with  $x = 0$ . For  $x < 0$ , the function  $\xi(1-x)/x = \eta$  is the dashed line reported in fig. 2. All the lines for  $x < 0$  go through the origin with the slope converging to the  $\eta$ -axis for  $x \rightarrow 0$ .

Given an  $x < 0$  and  $\xi + \eta > 0$ , the integration region is that in the lower half plane within the two lines  $\xi + \eta = 0$  and the dashed line. The integration directions must give a positive area, so a part of the integral on  $\eta$  is indicated in fig. 2 as a thick arrow. The contribution to  $F_2(x)$  of this part of the plane is  $F_2^a(x)$ :

$$F_2^a(x) = \int_{-\infty}^0 d\xi P_1(\xi) \int_{-\xi}^{\xi(1-x)/x} P_2(\eta) d\eta. \quad (4)$$

$P_1(\xi)$  and  $P_2(\eta)$  are the two distributions of the random variables  $\xi$  and  $\eta$ . The contribution to  $F_2(x)$  from the region with  $(\xi + \eta) < 0$  is given by the upper part of plane within the two lines  $\xi(1-x)/x = \eta$  and  $\xi = -\eta$ . A part of the integration path in  $\eta$  is indicated with a thick arrow in fig. 3.

Its contribution to  $F_2(x)$ , we call it  $F_2^b(x)$ , is given by:

$$F_2^b(x) = \int_0^{\infty} d\xi P_1(\xi) \int_{\xi(1-x)/x}^{-\xi} P_2(\eta) d\eta. \quad (5)$$

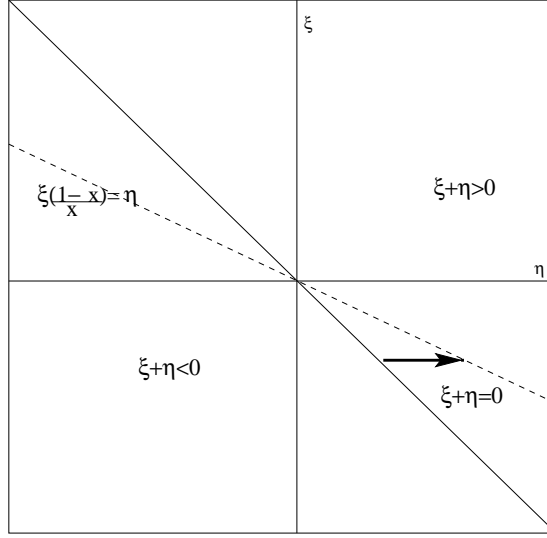


Figure 2: Sector of the plane  $(\eta, \xi)$  where  $\xi + \eta > 0$  or  $\xi + \eta < 0$  and its boundary  $\xi + \eta = 0$ , the dashed line is the line  $\xi(1-x)/x = \eta$  for negative  $x$ . The arrow indicates the integration path for  $(\xi + \eta) > 0$

For  $x > 0$  the lines are typically that reported in figure 4. Now we have to integrate on a larger sector. An integration must cover the region up to the line with  $x = 0$ , (the  $\eta$ -axis), and an integration must cover the remaining part up to the line  $\xi(1-x)/x = \eta$  for each  $(\xi + \eta) > 0$  and  $(\xi + \eta) < 0$ .  $F_2^c(x)$  and  $F_2^d(x)$  respectively for  $(\xi + \eta) > 0$  and  $(\xi + \eta) < 0$  are given by:

$$F_2^c(x) = \int_{-\infty}^0 d\xi P_1(\xi) \int_{-\xi}^{+\infty} P_2(\eta) d\eta + \int_0^{+\infty} d\xi P_1(\xi) \int_{\xi(1-x)/x}^{+\infty} P_2(\eta) d\eta \quad (6)$$

$$F_2^d(x) = \int_{-\infty}^0 d\xi P_1(\xi) \int_{-\infty}^{\xi(1-x)/x} P_2(\eta) d\eta + \int_0^{+\infty} d\xi P_1(\xi) \int_{-\infty}^{-\xi} P_2(\eta) d\eta$$

So for  $x \leq 0$  we obtain:

$$F_2(x) = \int_{-\infty}^0 d\xi P_1(\xi) \int_{-\xi}^{\xi(1-x)/x} P_2(\eta) d\eta + \int_0^{+\infty} d\xi P_1(\xi) \int_{\xi(1-x)/x}^{-\xi} P_2(\eta) d\eta \quad (7)$$

and  $x > 0$   $F_2(x)$  is:

$$F_2(x) = \int_{-\infty}^0 d\xi P_1(\xi) \int_{-\xi}^{+\infty} P_2(\eta) d\eta + \int_0^{+\infty} d\xi P_1(\xi) \int_{\xi(1-x)/x}^{+\infty} P_2(\eta) d\eta + \int_{-\infty}^0 d\xi P_1(\xi) \int_{-\infty}^{\xi(1-x)/x} P_2(\eta) d\eta + \int_0^{+\infty} d\xi P_1(\xi) \int_{-\infty}^{-\xi} P_2(\eta) d\eta \quad (8)$$

It is easy to verify the consistency of  $F_2(x)$ , in fact  $F_2(x \rightarrow -\infty) = 0$  and  $F_2(x \rightarrow +\infty) = 1$ . When  $x \rightarrow -\infty$  it is  $(1-x)/x \rightarrow -1$  and:

$$F_2(x \rightarrow -\infty) = \int_{-\infty}^0 d\xi P_1(\xi) \int_{-\xi}^{-\xi} P_2(\eta) d\eta + \int_0^{+\infty} d\xi P_1(\xi) \int_{-\xi}^{-\xi} P_2(\eta) d\eta = 0 \quad (9)$$

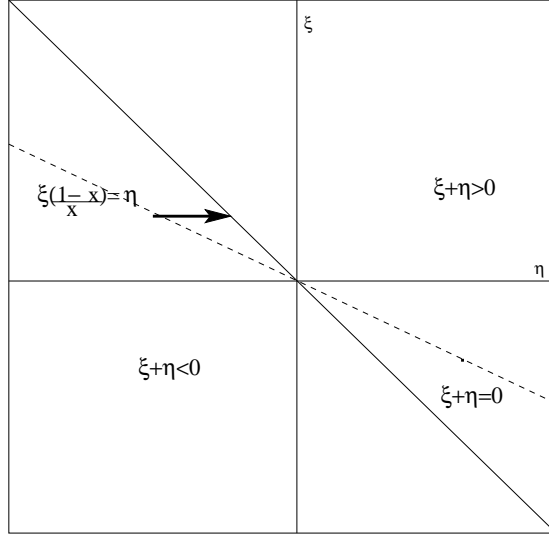


Figure 3: Sector of the plane  $(\eta, \xi)$  where  $\xi + \eta > 0$  or  $\xi + \eta < 0$  and its boundary  $\xi + \eta = 0$ , the dashed line is the line  $\xi(1-x)/x = \eta$  for negative  $x$ , the arrow indicates the  $\eta$  integration-path for  $(\xi + \eta) < 0$

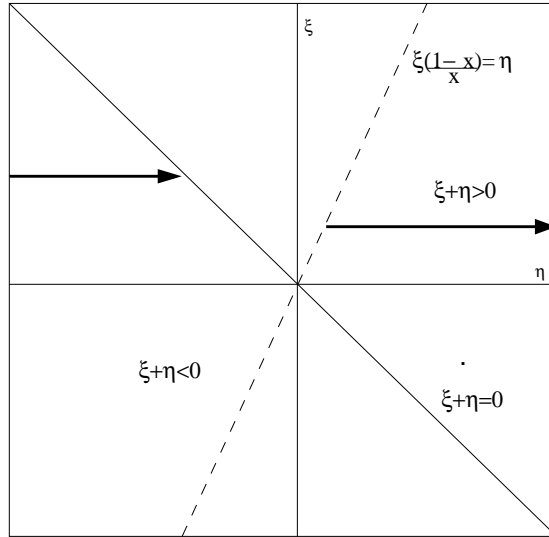


Figure 4: Sector of the plane  $(\eta, \xi)$  where  $\xi + \eta > 0$  or  $\xi + \eta < 0$  and its boundary  $\xi + \eta = 0$ , the dashed line is the line  $\xi(1-x)/x = \eta$  for positive  $x$ . The integration regions are that with the arrows and must cover positive and negative values of  $\xi$

the integration on  $\eta$  gives zero in the two integrals. For  $x \rightarrow +\infty$  and  $(1-x)/x \rightarrow -1$  it is:

$$\begin{aligned}
 F_2(x) &= \int_{-\infty}^0 d\xi P_1(\xi) \int_{-\xi}^{+\infty} P_2(\eta) d\eta + \int_0^{+\infty} d\xi P_1(\xi) \int_{-\xi}^{+\infty} P_2(\eta) d\eta + \\
 &\int_{-\infty}^0 d\xi P_1(\xi) \int_{-\infty}^{-\xi} P_2(\eta) d\eta + \int_0^{+\infty} d\xi P_1(\xi) \int_{-\infty}^{-\xi} P_2(\eta) d\eta \\
 &= \int_{-\infty}^{+\infty} P_2(\xi) d\xi \int_{-\infty}^{+\infty} P_1(\eta) d\eta = 1
 \end{aligned} \tag{10}$$

that is equal to one for the normalization of  $P_1$  and  $P_2$ . This check assures the absence of trivial errors.

## 2.1 Probability Density Function

The probability density function (PDF) is extracted by the function  $F_2(x)$  with a derivative respect to  $x$ . Due to the complex dependence from  $x$  of the boundaries of integration, the derivative must be done with the definition of an auxiliary variable  $y(x)$  and multiplying the derivative respect to  $y$  for  $dy/dx$ . We will indicate this PDF with  $P_{xg2R}(x)$ . The result is:

$$P_{xg2R}(x) = \frac{dF_2(x)}{dx} = \frac{1}{x^2} \left[ \int_0^{+\infty} d\xi P_1(\xi) \xi P_2\left(\xi \frac{1-x}{x}\right) - \int_{-\infty}^0 d\xi P_1(\xi) \xi P_2\left(\xi \frac{1-x}{x}\right) \right]. \quad (11)$$

An identical result is obtained differentiating  $F_2(x)$  for  $x \geq 0$  or  $F_2(x)$  for  $x < 0$ . Equation 11 is the PDF of the two strip COG assuming the independence of the two strip noise and the strip 1 is the right strip. The factor  $1/x^2$  and the factor  $\xi$  in the integral come from the derivative of  $\xi(1-x)/x$  respect to  $x$ .

To consider the left strip one can proceed as for the right strip obtaining different figures. The final result is equivalent to substitute to the probability  $P_1$  of the right strip the probability  $P_3$  of the left strip and change  $x$  in  $-y$  to obtain the PDF  $P_{xg2L}(y)$  of the two strip COG with the left strip.

## 2.2 Cumulative probability using the left strip

Even if the steps to obtain this distribution are identical to the previous ones, with a small modifications we will reproduce the path because it will be used in the following.

$$y = \frac{-\beta}{\beta + \eta} \quad (12)$$

As usual we calculate the function  $F_{2L}(y)$  defined as the region where  $-\beta/(\beta + \eta) < y$ . We have to separate the two regions  $\beta + \eta \geq 0$  and  $\beta + \eta < 0$  Now the integrals for  $y < 0$  has to be done as in fig.5

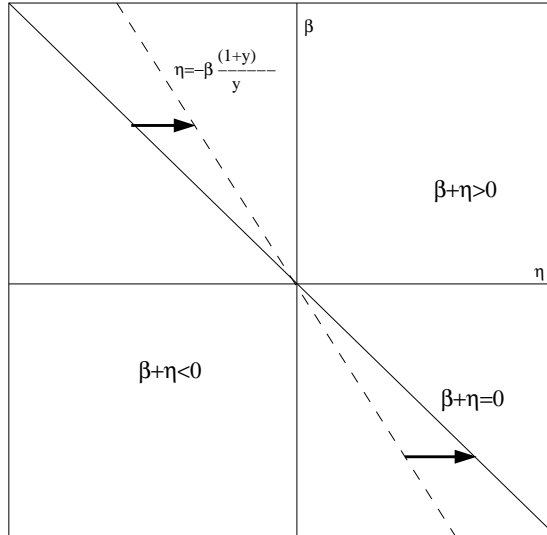


Figure 5: Integration regions for  $y < 0$  for the two strip COG with the left strip

The function  $F_{2L}(y)$  for  $y < 0$  is given by:

$$F_{2L}(y) = \int_0^{\infty} d\beta P_3(\beta) \int_{-\beta}^{\beta(-1-y)/y} P_2(\eta) d\eta + \int_{-\infty}^0 d\beta P_3(\beta) \int_{\beta(-1-y)/y}^{-\beta} P_2(\eta) d\eta \quad (13)$$

For  $y \geq 0$  the integration regions are that of fig. 6, obviously even above and below the  $\beta = 0$  line. The function  $F_{2L}(y)$  for  $y \geq 0$  is given by:

$$F_{2L}(y) = \int_0^{+\infty} d\beta P_3(\beta) \int_{-\beta}^{+\infty} P_2(\eta) d\eta + \int_{-\infty}^0 d\beta P_3(\beta) \int_{\beta^{(-1-y)/y}}^{+\infty} P_2(\eta) d\eta + \int_{-\infty}^0 d\beta P_3(\beta) \int_{-\infty}^{-\beta} P_2(\eta) d\eta + \int_0^{+\infty} d\beta P_3(\beta) \int_{-\infty}^{\beta^{(-1-y)/y}} P_2(\eta) d\eta \quad (14)$$

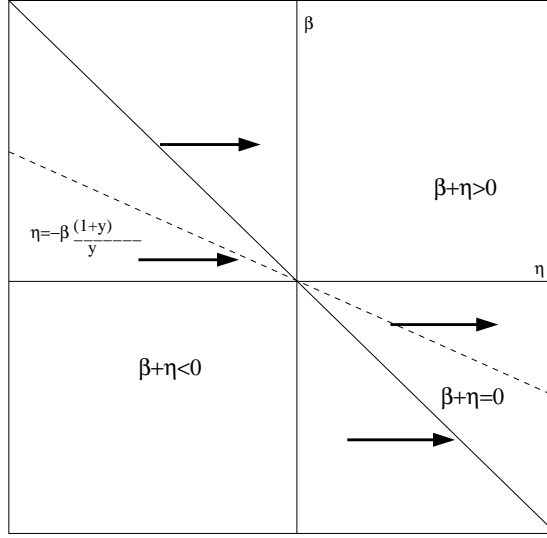


Figure 6: *Integration regions for  $y < 0$  for the two strip COG with the left strip*

To control the consistency of the equations, the limit of  $y \rightarrow \infty$  must give one. It is easy to verify this as in the approach of  $F_{2R}(x)$ .

Differentiating  $F_{2L}(y)$  respect to  $y$  gives the PDF for the COG distribution with the left strip.

$$P_{xg2L}(y) = \frac{1}{y^2} \left[ \int_0^{+\infty} d\beta P_3(\beta) \beta P_2\left(\frac{-1-y}{y} \eta\right) - \int_{-\infty}^0 d\beta P_3(\beta) \beta P_2\left(\frac{-1-y}{y} \beta\right) \right]. \quad (15)$$

The variables  $\beta, \xi, \eta$  can be approximated as an average value and an additive Gaussian noise. In this assumption the PDF  $P_1, P_2, P_3$  can be represented as Gaussian functions with averages corresponding to the unperturbed energy values collected by the strips. With MATHEMATICA [9], it is possible to obtain an exact form of the above integrals with Gaussian PDF. This full form is very complex, but we have to consider that we are interested in  $x$  or  $y$  values less than or equal to 0.5 in absolute value.

The full form of the PDF has a very unusual behavior for  $x \rightarrow \infty$ . It goes to  $\infty$  as  $constant/x^2$  with an extremely small constant ( $10^{-40}$ ). This convergence to  $\infty$  is very slow compared to a Gaussian function. The PDF has infinite variance and no average. Thus, for these PDF the central limit theorem cannot be applied. Numerical calculations does not reveal the divergence.

### 3 The complete two strip center-of-gravity

The equations developed up to now consider only two strips. The full two strip algorithm selects the second strip as the greatest of two (left and right) nearby strips. For  $x_g \approx 0$ , the noise can favor one or the other strip. So, the energy of the third strip can plays its role in generating the typical anomaly of the two strip COG. The addition of the third strip requires to study the function  $F_2(x)$  in three dimensions. The

combinations of the previous plots will be useful in this case. As in the previous sections, the three strips are indicated with the index 1 for the right strip, with the index 2 the central strip, and the index 3 with the left strip. The random variables are  $\xi$ ,  $\eta$  and  $\beta$  for the right, central and left strip and their axis are directed as  $y$ ,  $x$  and  $z$  axis of a 3D reference system . If the energy of the right strip is much higher than that of left strip, the effect of the left strip is negligible. At  $a_3 \rightarrow -\infty$  the calculation of  $F_2(x)$  is identical to that of fig. 2, 3, 4. When  $\xi \geq \beta$  one get eq. 7 and multiplies  $F_2$  by  $P_3(\beta)$  and limits the integrations to the due regions  $\xi \geq \beta$  as plotted in fig. 7.

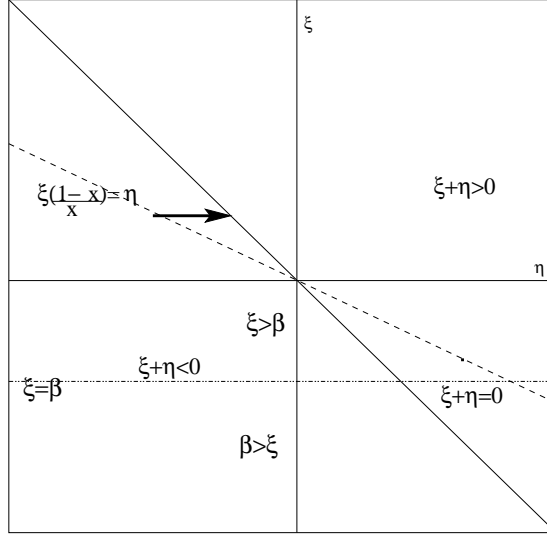


Figure 7: This is fig. 3 with the dash-dotted line indicating the boundary of the region with  $\xi \geq \beta$ . Now the integration region is above this line, here we have  $x < 0$ .

When  $\beta > \xi$  the function  $F_2(y)$  is used with the substitution  $y \rightarrow x$  and  $P_1(\xi) \rightarrow P_3(\beta)$  and integrating over the regions  $\beta \geq \xi$ . The result is:

$$x < 0$$

$$\begin{aligned}
F_3(x) = & \int_{-\infty}^0 d\beta P_3(\beta) \int_{\beta}^0 d\xi P_1(\xi) \int_{-\xi}^{\xi(1-x)/x} P_2(\eta) d\eta + \\
& \int_0^{\infty} d\beta P_3(\beta) \int_{\beta}^{\infty} d\xi P_1(\xi) \int_{\xi(1-x)/x}^{-\xi} P_2(\eta) d\eta + \\
& \int_{-\infty}^0 d\beta P_3(\beta) \int_0^{\infty} d\xi P_1(\xi) \int_{\xi(1-x)/x}^{-\xi} P_2(\eta) d\eta + \\
& \int_{-\infty}^0 d\xi P_1(\xi) \int_{\xi}^0 d\beta P_3(\beta) \int_{\beta(-1-x)/x}^{-\beta} P_2(\eta) d\eta + \\
& \int_0^{\infty} d\xi P_1(\xi) \int_{\xi}^{\infty} d\beta P_3(\beta) \int_{-\beta}^{\beta(-1-x)/x} P_2(\eta) d\eta \\
& \int_{-\infty}^0 d\xi P_1(\xi) \int_0^{\infty} d\beta P_3(\beta) \int_{-\beta}^{\beta(-1-x)/x} P_2(\eta) d\eta
\end{aligned} \tag{16}$$

The condition  $\lim_{x \rightarrow -\infty} F_3(x) = 0$  is easily verified due to the coincidence of the two integration limits of the inner integrals. The integration regions for  $x \geq 0$  are illustrated in fig. 8.

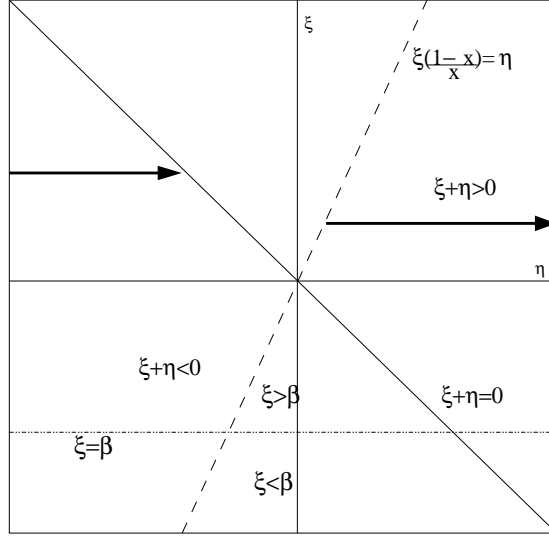


Figure 8: This is fig. 4 with the dash-dotted line indicating the boundary of the region with  $\xi \geq \beta$ . The integration region is above this line, here we have  $x > 0$ .

$$x \geq 0$$

$$\begin{aligned}
F_3(x) = & \int_{-\infty}^0 d\beta P_3(\beta) \int_{\beta}^0 d\xi P_1(\xi) \int_{-\xi}^{+\infty} P_2(\eta) d\eta + \int_0^{\infty} d\beta P_3(\beta) \int_{\beta}^{+\infty} d\xi P_1(\xi) \int_{\xi(1-x)/x}^{+\infty} P_2(\eta) d\eta + \\
& \int_{-\infty}^0 d\beta P_3(\beta) \int_{\beta}^0 d\xi P_1(\xi) \int_{-\infty}^{\xi(1-x)/x} P_2(\eta) d\eta + \int_0^{\infty} d\beta P_3(\beta) \int_{\beta}^{+\infty} P_1(\xi) d\xi \int_{-\infty}^{-\xi} P_2(\eta) d\eta + \\
& \int_0^{\infty} d\xi P_1(\xi) \int_{\xi}^{+\infty} d\beta P_3(\beta) \int_{-\beta}^{+\infty} d\eta P_2(\eta) + \int_{-\infty}^0 d\xi P_1(\xi) \int_{\xi}^0 d\beta P_3(\beta) \int_{\beta(-1-x)/x}^{+\infty} d\eta P_2(\eta) + \\
& \int_{-\infty}^0 d\xi P_1(\xi) \int_{\xi}^0 d\beta P_3(\beta) \int_{-\infty}^{-\beta} P_2(\eta) d\eta + \int_0^{\infty} d\xi P_1(\xi) \int_{\xi}^{+\infty} d\beta P_3(\beta) \int_{-\infty}^{\beta(-1-x)/x} P_2(\eta) d\eta + \\
& \int_{-\infty}^0 d\beta P_3(\beta) \int_0^{\infty} d\xi P_1(\xi) \int_{\xi(1-x)/x}^{\infty} d\eta P_2(\eta) + \int_{-\infty}^0 d\beta P_3(\beta) \int_0^{\infty} d\xi P_1(\xi) \int_{-\infty}^{-\xi} d\eta P_2(\eta) + \\
& \int_{-\infty}^0 d\xi P_1(\xi) \int_0^{\infty} d\beta P_3(\beta) \int_{-\beta}^{\infty} d\eta P_2(\eta) + \int_{-\infty}^0 d\xi P_1(\xi) \int_0^{\infty} d\beta P_3(\beta) \int_{-\infty}^{\beta(-1-x)/x} d\eta P_2(\eta)
\end{aligned} \tag{17}$$

This complex set of integrals are necessary to complete the integration space of the variables for  $F_3(x)$ , and they give the correct limits for  $x \rightarrow \pm\infty$  (in a first calculation the last four were lost and the limit for  $x$  going to  $\infty$  was wrong). It is required a transformation of the integrals on a triangular region with the Fubini's theorem.

The probability distribution is obtained with a derivative of eq. 17 in the  $x$  variable.

$$\begin{aligned}
P_{xg2}(x) = \frac{1}{x^2} & \left[ \int_0^\infty d\beta P_3(\beta) \int_\beta^\infty d\xi P_1(\xi) \xi P_2\left(\xi \frac{1-x}{x}\right) - \int_{-\infty}^0 d\beta P_3(\beta) \int_\beta^0 d\xi P_1(\xi) \xi P_2\left(\xi \frac{1-x}{x}\right) + \right. \\
& \int_0^\infty d\xi P_1(\xi) \int_\xi^\infty d\beta P_3(\beta) \beta P_2\left(\beta \frac{-1-x}{x}\right) - \int_{-\infty}^0 d\xi P_1(\xi) \int_\xi^0 d\beta P_3(\beta) \beta P_2\left(\beta \frac{-1-x}{x}\right) + \\
& \left. \int_{-\infty}^0 d\beta P_3(\beta) \int_0^\infty d\xi P_1(\xi) \xi P_2\left(\xi \frac{1-x}{x}\right) + \int_{-\infty}^0 d\xi P_1(\xi) \int_0^\infty d\beta P_3(\beta) \beta P_2\left(\beta \frac{-1-x}{x}\right) \right] \quad (18)
\end{aligned}$$

The first four integrals can be rearranged with the Fubini's theorem and summed with the last two integrals giving:

$$\begin{aligned}
P_{xg2}(x) = \frac{1}{x^2} & \left[ \int_0^\infty d\xi P_1(\xi) \xi P_2\left(\xi \frac{1-x}{x}\right) \int_{-\infty}^\xi d\beta P_3(\beta) - \right. \\
& \int_{-\infty}^0 d\xi P_1(\xi) \xi P_2\left(\xi \frac{1-x}{x}\right) \int_{-\infty}^\xi d\beta P_3(\beta) + \\
& \int_0^\infty d\beta P_3(\beta) \beta P_2\left(\beta \frac{-1-x}{x}\right) \int_{-\infty}^\beta d\xi P_1(\xi) - \\
& \left. \int_{-\infty}^0 d\beta P_3(\beta) \beta P_2\left(\beta \frac{-1-x}{x}\right) \int_{-\infty}^\beta d\xi P_1(\xi) \right] \quad (19)
\end{aligned}$$

that can be recast in:

$$\begin{aligned}
P_{xg2}(x) = \frac{1}{x^2} & \left[ \int_{-\infty}^\infty d\xi |\xi| P_1(\xi) P_2\left(\xi \frac{1-x}{x}\right) \int_{-\infty}^\xi d\beta P_3(\beta) + \right. \\
& \left. \int_{-\infty}^\infty d\beta |\beta| P_3(\beta) P_2\left(\beta \frac{-1-x}{x}\right) \int_{-\infty}^\beta d\xi P_1(\xi) \right] \quad (20)
\end{aligned}$$

This last form is easier to handle numerically or analytically. MATHEMATICA does not give an analytical form of the integrals with Gaussian probability distributions, erf-functions do not allow an analytical result. The numerical integrals have convergence problems around  $x \approx 0$  even if the results are excellent. The two separate regions of probability for  $x$  are perfect. The function requires three energies and three standard deviations to produce the results. The three energies should be the unperturbed ones but it is evident that these are impossible to have.

## 4 Three strip COG probability distribution

Around  $x_{g2} = 0$  we see an anomaly that produces an incorrect reconstruction of the impact point. In this region we can try to use the three strip COG algorithm. It has no singularity around  $x_{g3} = 0$  (it has singularities around  $x_{g3} = \pm 0.5$  [8]). Even if the noise is higher than the  $x_{g2}$  it could be convenient to test this strategy in a best fit. For this task it is required the probability distribution.

As for  $x_{g2}$  we have to work in a three dimensional space.

$$a_1 = \xi, \quad a_2 = \eta, \quad a_3 = \beta \quad x_{g3} = \frac{\xi - \beta}{\xi + \eta + \beta}$$

For  $\beta = 0$  and  $\xi + \eta > 0$  we have the plot of fig. 9 (identical to fig. 3) but now we have to explore the condition:

$$\frac{\xi - \beta}{\xi + \eta + \beta} < x. \quad (21)$$

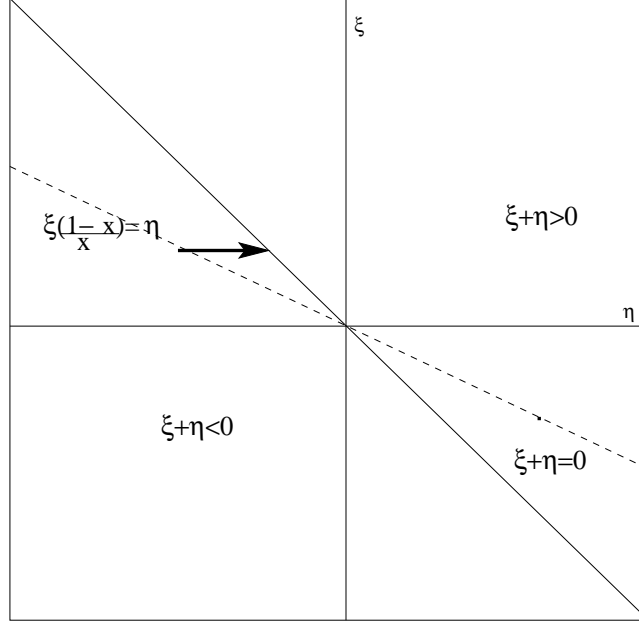


Figure 9: Sector of the plane  $(\eta, \xi)$  where  $\xi + \eta > 0$  or  $\xi + \eta < 0$  and its boundary  $\xi + \eta = 0$ , the dashed line is the line  $\xi(1-x)/x = \eta$  for negative  $x$ , the arrow indicates the  $\eta$  integration-path for  $(\xi + \eta) < 0$

We have two possibilities  $\xi + \eta + \beta > 0$  and  $\xi + \eta + \beta < 0$ , in any case we have two limiting planes:

$$\xi(1-x) + \beta(-1-x) - \eta x = 0 \quad \text{and} \quad \xi + \eta + \beta = 0$$

for  $x < 0$  and  $\beta = 0$ , the traces of these two planes in the plane  $\eta, \xi$  are those of fig. 9. Let us see the case with  $\beta > 0$  and  $\beta = b$ . The traces of the two planes are those of fig. 10. The intersection point is  $\{-2b, b\}$  and it changes with  $\beta$ . It is evident that the only change in moving from  $\beta > 0$  and  $\beta < 0$  is the intersection point that changes its sign, and each line of the plot moves parallel to itself. Than  $F_1^{xg^3}(x)$  becomes ( $x < 0$ ):

$$F_1^{xg^3}(x) = \int_{-\infty}^{\infty} d\beta P_3(\beta) \int_{\beta}^{\infty} d\xi P_1(\xi) \int_{\xi \frac{(1-x)}{x} + \beta \frac{(-1-x)}{x}}^{-\xi-\beta} P_2(\eta) d\eta + \int_{-\infty}^{\infty} d\beta P_3(\beta) \int_{-\infty}^{\beta} d\xi P_1(\xi) \int_{-\xi-\beta}^{\xi \frac{(1-x)}{x} + \beta \frac{(-1-x)}{x}} P_2(\eta) d\eta \quad (22)$$

For  $x \geq 0$  the traces of the two planes for  $\beta = 0$  are illustrated in fig. 4, and its identical fig. 11. With  $\beta \neq 0$  the traces of the two planes become these of fig. 12. The arrows indicate the integration paths. The intersection of the two lines are in the point  $\{-2b, b\}$  and the  $F_2^{xg^3}(x)$  becomes:

$$F_2^{xg^3}(x) = \int_{-\infty}^{\infty} d\beta P_3(\beta) \int_{-\infty}^{\beta} d\xi P_1(\xi) \int_{-\xi-\beta}^{\infty} P_2(\eta) d\eta + \int_{-\infty}^{\infty} d\beta P_3(\beta) \int_{\beta}^{\infty} d\xi P_1(\xi) \int_{\xi \frac{(1-x)}{x} + \beta \frac{(-1-x)}{x}}^{+\infty} P_2(\eta) d\eta + \int_{-\infty}^{\infty} d\beta P_3(\beta) \int_{-\infty}^{\beta} d\xi P_1(\xi) \int_{-\infty}^{\xi \frac{(1-x)}{x} + \beta \frac{(-1-x)}{x}} P_2(\eta) d\eta + \int_{-\infty}^{\infty} d\beta P_3(\beta) \int_{\beta}^{+\infty} d\xi P_1(\xi) \int_{-\infty}^{-\xi-\beta} P_2(\eta) d\eta \quad (23)$$

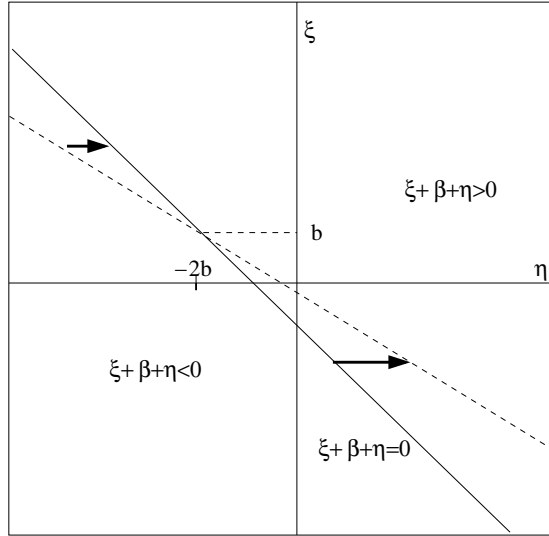


Figure 10: Sector of the plane  $(\eta, \xi)$  where  $\xi + \eta + \beta > 0$  or  $\xi + \eta + \beta < 0$  and its boundary  $\xi + \eta + \beta = 0$ , the dashed line has the equation  $\xi(1-x) + b(-1-x) - \eta x = 0$  for negative  $x$ , the arrows indicate the  $\eta$  integration-paths for  $(\xi + \eta + \beta) < 0$  and for  $(\xi + \eta + \beta) > 0$

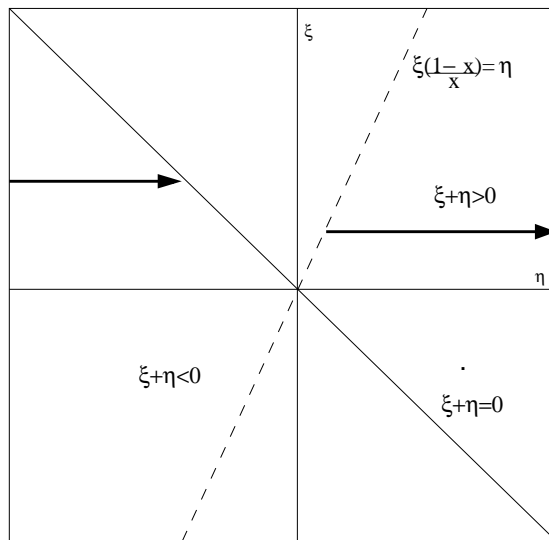


Figure 11: Sector of the plane  $(\eta, \xi)$  where  $\xi + \eta > 0$  or  $\xi + \eta < 0$  and its boundary  $\xi + \eta = 0$ , the dashed line is the line  $\xi(1-x)/x = \eta$  for positive  $x$ . The integration regions are that with the arrows and must cover positive and negative values of  $\xi$

It is easy to prove that  $\lim_{x \rightarrow -\infty} F_1^{xg^3}(x) = 0$  and  $\lim_{x \rightarrow +\infty} F_2^{xg^3}(x) = 1$ . In fact the first limit is easy given that  $\lim_{x \rightarrow \pm\infty} (1-x)/x = -1$ . With this position eq. 22 has the limits of the last integrals identical, and

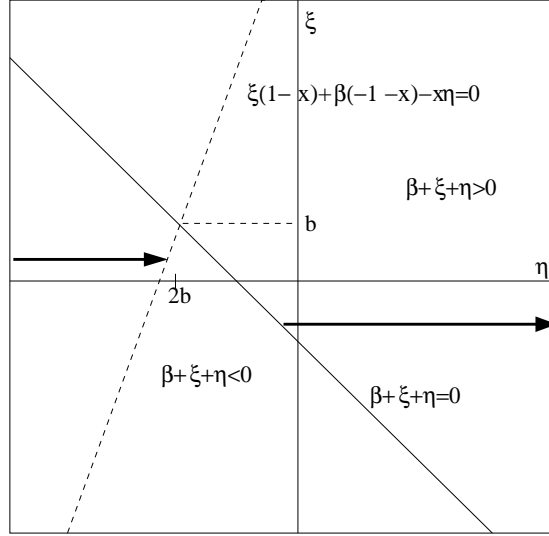


Figure 12: Sector of the plane  $(\eta, \xi)$  where  $\xi + \eta + \beta > 0$  or  $\xi + \eta + \beta < 0$  and its boundary  $\xi + \eta + \beta = 0$ , the dashed line is the line  $\xi(1-x) + \beta(-1-x) - x\eta = 0$  for positive  $x$ . The integration regions are that with the arrows and must cover positive and negative values of  $\xi$

the integrals are zero. For  $x \rightarrow +\infty$  the integrals of eq. 23 become:

$$\begin{aligned}
F_2^{xg3}(+\infty) &= \int_{-\infty}^{\infty} d\beta P_3(\beta) \int_{-\infty}^{\beta} d\xi P_1(\xi) \int_{-\xi-\beta}^{\infty} P_2(\eta) d\eta + \\
&\int_{-\infty}^{\infty} d\beta P_3(\beta) \int_{\beta}^{\infty} d\xi P_1(\xi) \int_{-\xi-\beta}^{+\infty} P_2(\eta) d\eta + \\
&\int_{-\infty}^{\infty} d\beta P_3(\beta) \int_{-\infty}^{\beta} d\xi P_1(\xi) \int_{-\infty}^{-\xi-\beta} P_2(\eta) d\eta \\
&\int_{-\infty}^{\infty} d\beta P_3(\beta) \int_{\beta}^{+\infty} d\xi P_1(\xi) \int_{-\infty}^{-\xi-\beta} P_2(\eta) d\eta
\end{aligned} \tag{24}$$

The first and third integrals have identical integration limits in the variables  $\beta$  and  $\xi$ , and the sum of the last integrals produces the normalization of the probability distribution  $P_2(\eta)$ . Identically for the second and fourth integrals. The two remaining integrals add completing the normalization of the probability  $P_1(\xi)$  that is multiplied by the normalization of  $P_3(\beta)$  giving 1.

Now, after this consistency check, we can extract the probability  $P_{xg3}(x)$  differentiating  $F_1^{xg3}(x)$  and  $F_2^{xg3}(x)$  respect to  $x$ . The result is:

$$\begin{aligned}
P_{xg3}(x) &= \frac{1}{x^2} \left[ \int_{-\infty}^{+\infty} d\beta P_3(\beta) \int_{\beta}^{+\infty} d\xi P_1(\xi) P_2\left(\xi \frac{1-x}{x} + \beta \frac{-1-x}{x}\right) (-\beta + \xi) + \right. \\
&\left. \int_{-\infty}^{+\infty} d\beta P_3(\beta) \int_{-\infty}^{\beta} d\xi P_1(\xi) P_2\left(\xi \frac{1-x}{x} + \beta \frac{-1-x}{x}\right) (\beta - \xi) \right]
\end{aligned} \tag{25}$$

With the transformation  $\delta = \xi - \beta$ , eq. 25 becomes:

$$\begin{aligned}
P_{xg3}(x) &= \frac{1}{x^2} \left[ \int_{-\infty}^{+\infty} d\beta P_3(\beta) \int_0^{+\infty} d\delta P_1(\delta + \beta) P_2\left(\delta \frac{1-x}{x} - 2\beta\right) \delta - \right. \\
&\left. \int_{-\infty}^{+\infty} d\beta P_3(\beta) \int_{-\infty}^0 d\delta P_1(\delta + \beta) P_2\left(\delta \frac{1-x}{x} - 2\beta\right) \delta \right]
\end{aligned} \tag{26}$$

or better:

$$P_{xg3}(x) = \frac{1}{x^2} \left[ \int_{-\infty}^{+\infty} d\beta P_3(\beta) \int_{-\infty}^{+\infty} d\delta P_1(\delta + \beta) P_2\left(\delta \frac{1-x}{x} - 2\beta\right) |\delta| \right] \quad (27)$$

That can be recast in a form more appropriate for the coming developments:

$$P_{xg3}(x) = \frac{1}{x^2} \left[ \int_{-\infty}^{+\infty} d\delta |\delta| \int_{-\infty}^{+\infty} d\beta P_3(\beta) P_1(\delta + \beta) P_2\left(\delta \frac{1-x}{x} - 2\beta\right) \right] \quad (28)$$

A set of variable transformations reports this form to be identical to equation 21 of ref. [1].

#### 4.1 Expression with Gaussian additive noise and few plots

With additive Gaussian noise, eq. 28 shows the possibility of an analytical expression of the integrals, in fact the integral on  $\beta$  is on product of Gaussian functions and it will give a Gaussian function. The integral on  $\delta$  has itself an analytical expression.  $P_{xg3}(x)$  assumes the form (with a consistent help of MATHEMATICA):

$$P_{xg3}(x) = \left\{ \exp \left[ - \left( \frac{a_1 - a_3}{a_1 + a_2 + a_3} - x \right)^2 \frac{(a_1 + a_2 + a_3)^2}{2[(1-x)^2 \sigma_1^2 + x^2 \sigma_2^2 + (1+x)^2 \sigma_3^2]} \right] \frac{a_1[x\sigma_2^2 + 2(1+x)\sigma_3^2] + a_3[2(1-x)\sigma_1^2 - x\sigma_2^2] + a_2[(1-x)\sigma_1^2 + (1+x)\sigma_3^2]}{\sqrt{2\pi}[(1-x)^2 \sigma_1^2 + x^2 \sigma_2^2 + (1+x)^2 \sigma_3^2]^{3/2}} \right\} \quad (29)$$

This form is simplified, with the suppression of elements with negligible contributions to the final result (as far as for the  $x$  values of our needs). We have an expression of the type  $A \operatorname{erf}(A)$  that is approximated as  $|A|$ . The differences with the full integral are really extremely small. The normalization of the distributions can be numerically verified in the range  $\approx \pm 3$ , beyond these values MATHEMATICA gives wrong a normalization due to the errors introduced by singularities in the integrands. These singularities are characteristic of the distributions of ratios of Gaussian random variables as shown in ref. [2].

Another form to write eq. 29 consists in the observation that the factors each  $\sigma_i$   $i = 1, 2, 3$  are the COG calculated with the exact energies in the reference system of the strip  $i$ . Defining  $X_3 = (a_1 - a_3)/(a_1 + a_2 + a_3)$ , we have:

$$\begin{aligned} a_1[x\sigma_2^2 + 2(1+x)\sigma_3^2] + a_3[2(1-x)\sigma_1^2 - x\sigma_2^2] + a_2[(1-x)\sigma_1^2 + (1+x)\sigma_3^2] = \\ (a_1 - a_3)x\sigma_2^2 + (2a_1 + a_2)(1+x)\sigma_3^2 + (2a_3 + a_2)(1-x)\sigma_1^2 = \\ (a_1 + a_2 + a_3)[X_3x\sigma_2^2 + (1+X_3)(1+x)\sigma_3^2 + (X_3 - 1)(x-1)\sigma_1^2] \end{aligned} \quad (30)$$

With the approximation  $X_3 \approx x$ , a further simplified form of eq. 29 can be obtained, this implies a small increase of the error (even in the normalization):

$$P_{xg3}(x) = \left\{ \exp \left[ - \left( \frac{a_1 - a_3}{a_1 + a_2 + a_3} - x \right)^2 \frac{(a_1 + a_2 + a_3)^2}{2(\sigma_1^2(1-x)^2 + x^2 \sigma_2^2 + (1+x)^2 \sigma_3^2)} \right] \frac{(a_1 + a_2 + a_3)}{\sqrt{2\pi} \sqrt{(\sigma_1^2(1-x)^2 + x^2 \sigma_2^2 + (1+x)^2 \sigma_3^2)}} \right\} \quad (31)$$

The following figure illustrates the probability reproduction of the data. With MATLAB [10], we generate a set of 500000 events all at the identical noiseless energy. The normalized histograms of  $x_{g2}$  and  $x_{g3}$  at  $\theta = 0^\circ$  and at a noiseless energy of 150 ADC five-strip energy are reported with the calculated probability distributions. The calculated distributions exactly overlaps the histograms.

The cumulative distributions for the complete three strip COG (with the gap at  $x \pm 1/2$  as illustrated in ref. [8]) will be reported in a coming paper.

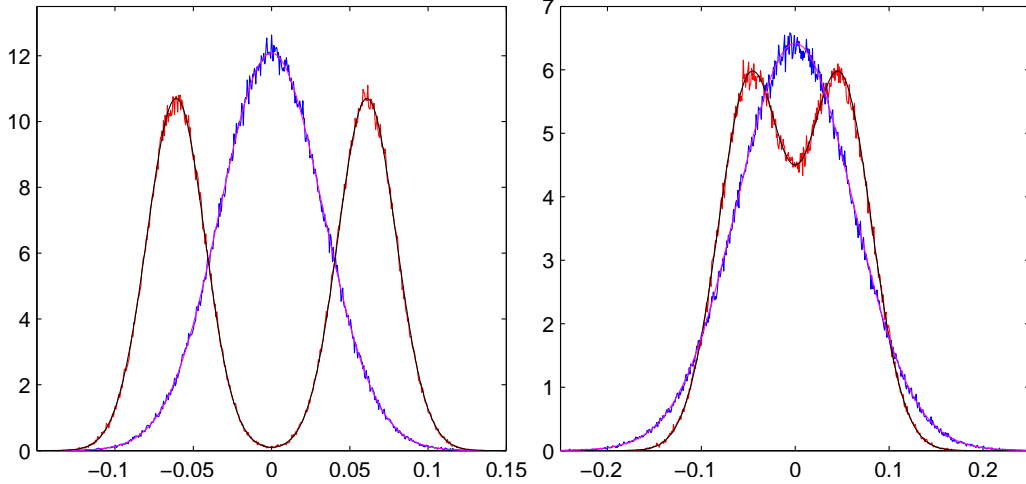


Figure 13: *Right plot. Simulation of the data distributions of  $x_{g2}$  in red and  $x_{g3}$  blue at the incidence angle  $\theta = 0^\circ$ , impact point  $\varepsilon = 0$  and noiseless energy 150 ADC counts (floating-strip detector). The black curve is the  $x_{g2}$  and the magenta one is the  $x_{g3}$  calculated probability distribution. Left plot. Simulations at  $\theta = 0^\circ$ ,  $\varepsilon = 0$  and noiseless energy 150 ADC for normal-strip detector with higher noise (6.5ADC)*

## 5 Conclusions

The probability distributions for the center-of-gravity as positioning algorithms are calculated with the textbook method with the cumulative probability. This method is very cumbersome but it is reported for completeness. This method was the first, we used long time ago, for this type of calculations. Other faster methods are reported in another previous report. Other type of center-of-gravity algorithms will be discussed in Part II.

## References

- [1] Landi G.; Landi G. E.; *Probability Distributions of Positioning Errors for Some Forms of Center-of-Gravity Algorithms*. arXiv:2004.08975 [physics.ins-det]
- [2] B. V. Gnedenko "The Theory of Probability and Elements of Statistics" (AMS Chelsea Publishing -Providence Rhode Island )
- [3] Landi G.; Landi G. E. *The Cramer-Rao inequality to go beyond the  $\sqrt{N}$ -limit of the standard least-squares method in track fitting* arXiv:1910.14494 [physics.ins-det] <https://arxiv.org/abs/1910.14494>.
- [4] Landi G.; Landi G. E. *Proofs of non-optimality of the standard least-squares method for track reconstructions* arXiv:2003.10021 [physics.ins-det]
- [5] Landi G.; Landi G. E. *Beyond the  $\sqrt{N}$ -limit of the least squares resolution and the lucky-model* arXiv:1808.06708[physics.ins-det] <https://arxiv.org/abs/1808.06708>.
- [6] Landi G.; Landi G. E. *Improvement of track reconstruction with well tuned probability distributions* JINST 9 2014 P10006. arXiv:1404.1968[physics.ins-det] <https://arxiv.org/abs/1404.1968>

- [7] Landi, G.; Landi G. E. *Optimizing momentum resolution with a new fitting method for silicon-strip detectors* INSTRUMENTS **2018**, 2, 22
- [8] Landi G., *The center of gravity as an algorithm for position measurements* Nucl. Instr. and Meth. A **485** (2002) 698 arXiv:1908.04447 [physics.ins-det] <https://arxiv.org/abs/1910.04447>.
- [9] Wolfram Research, Inc., MATHEMATICA, Version 6, Champaign, IL, USA
- [10] MATLAB 8, The MathWork, Inc., Natic, MA, USA